Imaging Bacterial Colonies and Phage-bacterium Interaction at Sub-nanometer Resolution Using Helium Ion Microscopy

*Miika Leppänen, Lotta-Riina Sundberg, Elina Laanto, Gabriel Magno de Freitas Almeida, Petri Papponen and Ilari J. Maasilta**

M. Leppänen, Prof. I. J. Maasilta
Nanoscience Center, Department of Physics, University of Jyvaskyla, P. O. Box 35, FI-40014 Jyväskylä, Finland
E-mail: ilari.j.maasilta@jyu.fi

M. Leppänen, Dr. L.-R. Sundberg, Dr. E. Laanto, Dr. G.M.F. Almeida, P. Papponen
Nanoscience Center, Center of Excellence in Biological Interactions, Department of Biological and Environmental Science, University of Jyvaskyla, FI-40014 Jyväskylä, Finland

Imaging of microbial interactions has so far been based on well-established electron microscopy methods. Here we present a new way to study bacterial colonies and interactions between bacteria and their viruses, bacteriophages (phages), in-situ on agar plates using helium ion microscopy (HIM). In biological imaging, HIM has advantages over traditional scanning electron microscopy with its sub-nanometer resolution, increased surface sensitivity, and the possibility to image non-conductive samples. Furthermore, by controlling the He beam dose or by using heavier Ne ions, the HIM instrument provides the possibility to mill out material in the samples, allowing for sub-surface imaging and in-situ sectioning. Here, we present the first HIM-images of bacterial colonies and phage-bacterium interactions at different stages of the infection as they occur on an agar culture. We also demonstrate the feasibility of neon and helium milling to reveal the sub-surface structures of bacterial colonies on agar substrate, and in some cases also structure inside individual bacteria after cross-sectioning. We conclude that helium ion microscopy offers great opportunities to advance the studies of microbial imaging, in particular in the area of interaction of viruses with cells.

1. Introduction

Helium ion microscope (HIM) is a recently developed scanning microscopy tool, which utilizes a positively charged He+ or Ne+ ion beam for imaging and nanopatterning.[1-3] It resembles scanning electron microscopy (SEM) in the sense that the raster scanned beam excites secondary electrons from the surface region of the specimen, and these electrons, whose emission is sensitive to surface topography, form the image. Compared to the best modern SEMs, the probe size can be up to five times smaller down to a diameter ~0.3 nm, and the probe-sample surface interaction volume is also much reduced due to the much heavier mass of the ions.[2] Both of these factors result in a higher imaging resolution, ultimately limited by the probe size. In addition, the depth of focus is about five times larger, as well.[2] Even more importantly for biological imaging, a conductive coating isn't required at all in HIM so that fragile sub-nanometer structures in a native state can be imaged with HIM without masking or artefacts due to the coating.[4]

So far, nanoscale features have been imaged with HIM mostly in mammalian cells, such as human colon cancer cells,[5] human liver cells,[6] rabbit cartilage collagen networks,[7] HeLa cells,[4] rat kidney,[8] rat and mouse epidermis,[9] and human neural stem cells, neurons and mouse neurons.[10] Many of these studies have shown that uncoated samples reveal more ultrastructures than coated samples. Outside of the mammalia, HIM has been used to image scales of lepidoptera (butterfly) wings[11] and cuticle structures in Drosophila.[12] The study by Joens *et al*[4] included also examples of imaging of a plant (*Arabidopsis thaliana*), a nematode (*Pristionchus pacificus*), and nitrate reducing *Acidovorax sp*. bacteria. Apart from that lone study, HIM microscopy of microbes has not been pursued before this work, where our aim was to explore the nanoscale imaging capacity of HIM for microbiological samples; for bacteria and their viruses.

Bacteriophages (phages), the viruses infecting bacteria, can cause lethal infections in their bacterial hosts, thus participating in global biogeochemical processes that involve bacteria.[13, 14] Phage infection occurs when a phage binds to specific structures on the surface of its host bacterium (outer membrane proteins, lipopolysaccharides, pili or flagella etc.) and injects its genome. In tailed phages[15], the binding in the host is mediated by the tail fibers of the phage. After binding, the phage injects its genome inside the bacterial cell in a syringe-like manner, which results in conformational changes and shortening of the phage tail in phages of the family *Myoviridae*.[16] During the lytic cycle, new phage particles are then produced inside the infected cell, and eventually released into the surroundings upon eruption and death of the host.

While these general steps in the life cycle of the phage are relatively well known, the imaging of bacterial cells and their phages has remained challenging and has been restricted by the resolution limits and complexity of commonly used microscopy techniques. Scanning electron microscopy (SEM) has provided details on bacterial surface structures and phage-bacterium interactions[17], but it requires that the sample is coated with a metal (e.g. gold, platinum), which typically leads to the loss of resolution and artefacts in the smallest scale ultrastructures. Transmission electron microscopy (TEM) methods are currently the most widely used methods to study bacteria-phage interaction at high resolution. There, requirements for the sample preparation limit the feasibility of TEM for studying interaction in natural microbial communities. Recently, atomic force microscopy (AFM) has also been applied to image phage-bacterium interactions.[18,19]

In addition to imaging, by increasing the He dose or by changing to the heavier Ne ions, HIM can also be used to modify the sample by “milling” off material from a wanted area. Most milling applications have so far been in materials science applications[2, 3] with very little

biological work. The only example of HIM milling of a biological sample we are aware of is that of Joens *et al.*,[4] where a membranous sheath of the mouth of a nematode was cut out using Ne to reveal structures inside it. On the other hand, ion beam milling in combination with biological cellular imaging is already widely used using the more mature FIB-SEM dual beam instruments, where a Ga ion beam is used for milling to expose new cross-sectional surfaces to be imaged by a standard SEM column.[20] Compared to HIM, this technique suffers from an order of magnitude lower milling resolution due to the larger sample-beam interaction volume, in addition to the degraded SEM imaging capabilities and sensitivities to charging artefacts. Moreover, delicate biological samples are typically encased in a protective resin for FIB-SEM 3D-imaging.

In this work, we present the first HIM images of bacteria-phage interactions at various stages of the infection, at sub-nm imaging resolution. We also investigate the possibilities to mill and image microbial samples with HIM, without any protective resins or coatings, made possible because of the more gentle nature of the HIM milling. Subsurface *E. coli* microcolonies inside an agar plate were imaged after milling a view-through hole. In addition, individual bacterial cross-sections were performed.

2. Results and discussion

2.1. HIM imaging of phage-bacterium interaction

The sample containing viral plaques formed by the phage T4 on the *E. coli* bacterial lawn on agar was first investigated with an optical microscope to map out areas for HIM-studies, with one ~700 µm diameter plaque shown in **Figure 1** both optically (Figure 1a) and with the HIM (Figure 1b). The diffuse plaque borders seen in the optical image are also visible in the HIM image as changing morphology (Figure 1b). To visualize various stages of the T4 infection,

we explored different regions of the plaque. These regions represent different temporal phases of the infection, because the center of the plaque is the origin of the infection, from which the phage multiplication spreads out radially.

Close ups of region 1 are shown in **Figure 2**, first in an area ~17 µm x 17 µm (Figure 2a), with a further zoom-in of a 2.6 µm x 2.6 µm region (Figure 2b). This kind of zooming into the nanoscale is quite easy with the HIM during an imaging session, facilitating the searching of most interesting regions from a large area samples. From Figure 2a we see that the central region of the plaque is almost free from bacteria, as the infection has already killed most of the bacteria and spread out. In the higher, nanoscale resolution image, Figure 2b, some phages can be seen lying on the agar surface.

By proceeding outwards along the direction of the spread of the infection to region 2 in Figure 1b, which is closer to the edge of the plaque, we find active infections, as shown in more detail in **Figure 3**. Figure 3a shows a ~ 13 µm x 13 µm image of several micron-scale *E. coli* bacteria, with all of them having phages attached on their surfaces. No bacteria have managed to avoid the infection. The zoomed-in image of Figure 3b (area 1.5 µm x 1.5 µm) shows three infected bacteria with multiple phages on each of them. With this magnification, the tailed morphology of the phage is clearly visible. Even more notably, we can compare within this same image the tails of phages that either are or are not attached to the bacteria. The length of the tail of the non-attached phages can be as long as ~100 nm, whereas some of the phages connected to the bacterial cell wall show much more contracted tails, indicating genome injection in progress.

Finally, at the edge of the plaque there are numerous bacterial cells, as they are in a stationary growth phase as a colony (**Figure 4**). Phage infection is much rarer, however, some ongoing

infections are still visible. There is also an exceptionally long *E. coli* cell shown in Figure 4, which are only recently described.[21]

To further highlight the abilities of HIM imaging of bacteriophages and their interactions with bacterial cells, we discuss additional details observed from the images. As already pointed out, different stages of infection were seen at different locations. An example of a high resolution image of a T4 phage anchored on the cell surface at an early stage is shown in **Figure 5**a. In this image, as in others, the icosahedral shape of the head capsid of the phage is clearly visible. In the active infection stage shown in high resolution in Figure 5b, the tails of the phages are clearly contracted down to lengths ~ 25 nm. Additional details can also be seen. For example, the image shows a widening of the end of the tail due to the baseplate structure, and even the tail fibers attached on the bacterial cell surface are visible, with fiber diameters in the range of a few nm. In Figure 5c, on the other hand, we likely see an example of the last stage of the infection, where new phage particles have burst out from a bacterium.

In all the images discussed above, the dried agar gel matrix structure in the background could be imaged with fiber widths down to the nanometer scale. In its important to point out that the smallest scale fragile structures such as the thinnest agar fibers and the thinnest phage tail fibers could not be resolved anymore if a thin gold metal coating was used on the samples (as is typically necessary with SEM). In addition, we sometimes observed broken agar fibers in the gold coated samples (not shown), whereas in the non-coated, directly HIM imaged samples broken fibers were never seen.

2.2. HIM-imaging of interactions between bacterial cells

As an additional example of the power of biological HIM imaging, we also show examples of visualizing interactions between bacterial cells of another bacterial species, the fish pathogen *Flavobacterium columnare*, on an agar plate culture. Images of a *F. columnare* B185 colony growing on an agar plate are shown in **Figure 6**. In addition to the bacterial cells, a lot of extracellular material such as round vesicles and nanoscale fibers between bacteria are found in the colony. Figure 6a also demonstrates the high depth of view available in a helium ion microscope, as the image is sharp everywhere even though the sample stage was tilted 45º (top and bottom of the image at different distances from the objective). In this particular case the depth of view was thus over 16 µm. In the higher resolution image, Figure 6b, we focused on the edge of the colony, where the interaction between the bacterial cells and the agar substrate network can clearly be seen. Extracellular, straight, thin fibers of nanometer scale are seen to emanate from the bacterial cell bodies, which the bacteria seem to utilize to attach to the underlying agar surface. Similar fibers also connect from bacteria to other bacteria, better seen in Figure 6a. In addition, small nanoscale membrane vesicles[22] are visible in several bacteria. Again, a metal coating of the samples can be very detrimental, possibly destructive to these smallest structures.

2.3. Helium milling

By increasing the He ion current, the He ions can start milling out softer materials. This possibility was tested on agar substrate samples, by drawing shapes with the pattern generator of our HIM setup. Initial tests using a current of 3 pA led to massive rupturing and cracks hundreds of micrometers long on the agar substrate, possibly because of local charge buildup issues. This problem was remedied by performing the milling with the floodgun on in the linescan mode. With a milling current 3 pA and a 3 minute exposure time, a square shaped

hole of size 100 nm x 100 nm was formed in the agar (**Figure 7**a) without any rupturing problems.

Helium milling was done also on the *E. coli* bacterial culture containing the T4 phage, with the idea of making a cross-sectional cut of a bacterial cell. During the milling, a current of 10 pA and a dwell time of 10 µs were used, with the flood gun on. In this case, the sample stage was tilted by 45 degrees, and the milling was performed layer-by-layer by moving a reduced-raster line scan view to the desired position. This way, monitoring of the milling process in real time is possible, and charge compensation prevents unwanted disruptions. The total milling time in this test was about 5 minutes. After milling the sample, the stage was rotated by 180º and the sectioned surface was imaged. An example of a cross-sectioned bacterium with a half-cut phage particle on it is shown in Figure 7b. The cross-sectional surface of the bacterium is smooth with no internal details. On can also see modified ("melted") phage particles in the right-bottom corner where the beam has hit.

Helium milling was done also to a *Flavobacterium sp.* B183 lying on a silicon substrate. Single lines were drawn by the pattern generator cross-sectionally over the bacterial body, the exposure was done with a dose 2 nC/µm^2, a current 1.272 pA and a total exposure time of 55 s. Flood gun use was not necessary because the charging effect is much weaker on a silicon substrate. After the exposure, sharp and narrow cut-out sections are found (**Figure 8**a). To remove the separated "head" section of the cell seen in Figure 8a, a pattern was drawn over it with a dose 3 nC/ µm^2 and the same current 1.272 pA, resulting in total exposure time of 186 s. After this second exposure, the "head" part disappeared, and interestingly, some inner structural details of the bacterium became visible on the remaining cut out surface (Figure 8b). Note also how the Si substrate under the area of milling is protruding. This bubble formation

is a common result seen with HIM on silicon substrates[2], and results from helium having been trapped inside the silicon lattice.

2.4. Neon milling

Neon milling was tried on the sample containing *E.coli* and T4-phage on an agar substrate. With the heavier Ne ions, milling is faster and thus larger areas can be milled, with a trade-off of decreased resolution. A slot with a size 13x5 micrometers was milled with a 35 pA Ne beam in 45 minutes from a 45º angle. It was imaged from a 90º angle (looking straight down) with Ne as the imaging ion, as well, see **Figure 9**a. Bacterial colony is clearly seen to grow inside of the agar matrix. In this figure, the black regions represent areas, from where no secondary electrons can reach the detector because of shading. For that reason, the slot was imaged also by tilting the sample 45 degrees and by rotating by 90 degrees, see Figure 9b, providing a better view of the trench. With the help of the milling, we can therefore conclude that we can image portions of the colony under the agar surface, as well.

3. Conclusion

We have demonstrated that helium ion microscopy is a powerful tool to study bacterial colonies and bacteria-phage interactions on a natural agar growth substrate. This is the first time that such a high resolution imaging of an infecting virus attached to the host cell is imaged, at different stages of the infection, as it happens on an agar plate. The main advantages of HIM imaging over the related standard scanning electron microscopy technique are the higher depth of view, the lack of the need of metal coating and improved resolution. In addition, by increasing the current or by switching from He to Ne ions, samples can be milled in situ to expose sub-surface features, or milling can be used for cross-sectioning single cells

or even single virus particles. More understanding is still required on how to best perform the cross-sectional milling, as we saw in this work that sometimes image contrast on the cross sectional surface was lost. Tentative reasons for this could be redeposition of the milled out material or modification due to heating. What is promising about HIM milling is that the milling can be done in a point-and-shoot mode, at sub-nanometer resolution, without the typical and restricting resin embedding techniques often used with focused gallium ion beam milling (FIB) of biological samples in FIB- instruments.[20]

Naturally, it is possible also to compare HIM to other advanced biological imaging techniques. Higher resolution can be achieved with transmission electron microscopy (TEM), and it has been a standard method for the characterization of novel bacteriophage species for a long time.[23] With the addition of advanced image reconstruction techniques for sets of particles, cryo-electron microscopy methods can used to resolve virus structures down to below 4 Å.[24,25] However, because of the transmission principle, the required thin sectioning cause limitations in many cases, and the focus is typically in single cell and virus level imaging. HIM, in contrast, does not require any sectioning and can be applied directly to complex specimens of bacterial colonies without any image reconstruction methods. Another possibility is to use atomic force microscopy (AFM), which has been applied for imaging of viruses and virus-cell interactions,[18,19,26] but not nearly to the extent of electron microscopy. It can image samples in air or even in a wet environment and provides quantitative height information, but has a limited dynamic range perpendicular to the scanning direction, is not straightforward to implement for soft biological samples, and suffers often from tip contamination. HIM seems to offer a higher resolution, has a much higher depth of view and can image bacterial samples on irregular, non-flat substrates. Compared to TEM and AFM and cryo-EM, HIM is a more straightforward technique to use, providing information at various length scales, on whole colonies of microbes and interactions between the microbes

and the substrate, and interactions between the microbes and their viruses, all together in one image, down to sub-nm resolution.

4. Experimental Section

Bacterial cultures

To study the phage-bacterium interaction we used *Escherichia coli* (DSM613) and its phage T4 (DSM4505) obtained from DSMZ GmbH (Braunschweig, Germany), *Flavobacterium columnare* B185,[27] and *Flavobacterium sp.* B183.[28] The bacteria and the phages were cultured either in a lysogeny broth (LB) medium (*E. coli*) or in a Shieh-medium (*Flavobacterium*). Phage infecting cultures were prepared by first making double agar plates containing *E. coli* (300 microliters of a 4h turbid *E. coli* culture added to 3ml of soft LB agar, mixing, and then pouring on top of a LB agar plate). After that, 10 microliter drops of a dilution series of our T4 stock were added to plates, which were incubated overnight at room temperature until clear plaques on the bacterial lawns could be seen. A plate with individual plaques was selected for imaging. In addition, a silicon chip containing bacteria B183 was prepared by incubating the chip in a liquid culture overnight at room temperature, containing only bacteria.

Sample preparation

Pieces of approximately 5 mm x 5 mm size were cut from the agar plates, glued to glass coverslips with epoxy and left to adhere for 20 minutes. Next, the samples were incubated for 5h in a fixative containing 2 % glutaraldehyde in a 0.1 M sodium cacodylate (NaCac) buffer (pH 7.4). The samples were then washed with a 0.1 M NaCac buffer and incubated with 1% OsO_4 in 0.1 M NaCac for 30 min, after which the washing with 0.1 M NaCac was repeated.

After fixation, the samples were dehydrated in absolute ethanol (99.5%) with a step series (50%, 70%, 95%, 99.5%, 99.5%). The final drying from ethanol was done with a Bal-Tec CPD 030 critical point dryer. The dried samples were attached to metal stubs with the carbon tape for HIM-imaging. A silicon chip containing the *flavobacterium* B183 was prepared in a similar manner, expect that the CPD drying protocol was replaced by a hexamethyldisilazane (HMDS) drying. In that case, after the ethanol series, ethanol was replaced by HMDS via an intermediate 50/50 ethanol-HDMS mixture. The final HDMS solution was let to evaporate overnight.

HIM imaging and milling

Samples ware first investigated with optical microscope (Olympus BX51M) to find out interesting spots for HIM-studies. The helium ion microscope used was the Zeiss Orion Nanofab at the University of Jyväskylä Nanoscience Center cleanroom. For imaging, acceleration voltage of 30 kV and an aperture 10 µm was used. The spot size was varied between 5 and 6 to obtain an ion current in the range 0.3-0.7 pA. As all samples studied were non-conductive, the flood gun charge compensation was used, together with line averaging with 16 or 32 lines and a 0.5 or 1 µs dwell time.

Milling with helium was done by changing the spot size to 2 or 3, to increase the current to 3-9 pA, with milling patterns produced by the ELPHY Multibeam pattern generator (Raith GmbH, Dortmund, Germany) of our HIM setup. In addition, high current neon milling was performed with a 70 µm aperture and spot size 2 to obtain current of 30-40 pA. Neon imaging was performed with a 20 µm aperture and a spot size 7, with current 0.3-0.7 pA.

Acknowledgements

This work was supported by the Finnish Centre of Excellence Program of the Academy of Finland; the CoE in Biological Interactions 2012-2017 (#252411), by Academy of Finland grant #266879, and by Jane and Aatos Erkko Foundation, and by the Academy of Finland FIRI2014 infrastructure programme. We acknowledge technical guidance by K. Arstila.

References

[1] B. W. Ward, J. A. Notte, N. P. Economou, *Journal of Vacuum Science & Technology B.* **2006**, 24, 2871.

[2] R. Hill, J.A. Notte, L. Scipioni in *Chapter 2 - Scanning Helium Ion Microscopy*, Vol. 170 (Ed.: Peter W. Hawkes), Elsevier, **2012**, pp. 65-148.

[3] G. Hlawacek, V. Veligura, R. van Gastel, B. Poelsema, *J.Vac.Sci.Technol.B Nanotechnol.Microelectron.* **2014**, 32, 020801.

[4] M. S. Joens, C. Huynh, J. M. Kasuboski, D. Ferranti, Y. J. Sigal, F. Zeitvogel, M. Obst, C. J. Burkhardt, K. P. Curran, S. H. Chalasani, L. A. Stern, B. Goetze, J. A. J. Fitzpatrick, *Sci.Rep.* **2013**, 3, 3514.

[5] D. Bazou, G. Behan, C. Reid, J. J. Boland, H. Z. Zhang, *J. Microsc.* **2011**, 242, 290.

[6] X. Chen, C. N. B. Udalagama, C. Chen, A. A. Bettiol, D. S. Pickard, T. Venkatesan, F. Watt, *Biophys. J.* **2011**, 101, 1788.

[7] W.S. Vanden Berg-Foels, L. Scipioni, C. Huynh, X. Wen, *J. Microsc.* **2012**, 246, 168.

[8] W. L. Rice, A. Van Hoek N., T. Paunescu G., C. Huynh, B. Goetze, B. Singh, L. Scipioni, L. A. Stern, D. Brown, *PLoS One.* **2013**, 8, e57051.

[9] T. Paunescu G., W. W. C. Shum, C. Huynh, L. Lechner, B. Goetze, D. Brown, S. Breton, *Mol. Hum. Reprod.* **2014**, 20, 929.

[10] M. Schurmann, N. Frese, A. Beyer, P. Heimann, D. Widera, V. Mönkemöller, T. Huser, B. Kaltschmidt, C. Kaltschmidt, A. Gölzhäuser, *Small.* **2015**, 11, 5781.

[11] S. A. Boden, A. Asadollahbaik, H. N. Rutt, D. M. Bagnall, *Scanning.* **2012**, 34, 107.

[12] A. Boseman, K. Nowlin, S. Ashraf, J. Yang, D. Lajeunesse, *Micron.* **2013**, 51, 26.

[13] R. W. Hendrix, *Theor. Popul. Biol.* **2002**, 61, 471.

[14] C. A. Suttle, *Nat.Rev.Microbiol.* **2007**, 5, 801.

[15] H. -. Ackermann, *Res. Microbiol.* **2003**, 154, 245.

[16] P. G. Leiman, M. M. Shneider, *Adv. Exp. Med. Biol.* **2012**, 726, 93.

[17] G. Wendelschafer-Crabb, S. L. Erlandsen, D. H. Walker, *J. Virol.* **1975**, 15, 1498.

[18] E. V. Dubrovin, A. V. Popova, S. V. Kraevskiy, S. G. Ignatov, T. E. Ignatyuk, I. V. Yaminsky, N. V. Volozhantsev, *PLoS One.* **2012**, 7, e47348.

[19] E. V. Dubrovin, A. G. Voloshin, S. V. Kraevsky, T. E. Ignatyuk, S. S. Abramchuk, I. V. Yaminsky, S. G. Ignatov, *Langmuir.* **2008**, 24, 13068.

[20] K. Narayan, S. Subramaniam, *Nat Meth.* **2015**, 12, 1021.

[21] Z. W. El-Hajj, E. B. Newman, *J. Bacteriol.* **2015**, 197, 1507.

[22] E. Laanto, R. K. Penttinen, J. K. H. Bamford, L. Sundberg, *BMC Microbiol.* **2014**, 14, 170.

[23] H. W. Ackermann, *Adv. Virus Res.* **2012**, 82, 1.

[24] N. M. Taylor, N. S. Prokhorov, R. C. Guerrero-Ferreira, M. M. Shneider, C. Browning, K. N. Goldie, H. Stahlberg, P. G. Leiman, *Nature.* **2016**, 533, 346.

[25] K. K. Lee, L. Gui, *PLoS Pathog.* **2016**, 12, e1005625.

[26] Y. G. Kuznetsov, A. McPherson, *Microbiol. Mol. Biol. Rev.* **2011**, 75, 268.

[27] E. Laanto, J. K. H. Bamford, J. J. Ravantti, L. Sundberg, *Front.Microbiol.* **2015**, 6, 829.

[28] E. Laanto, L. R. Sundberg, J. K. Bamford, *Appl. Environ. Microbiol.* **2011**, 77, 7868.

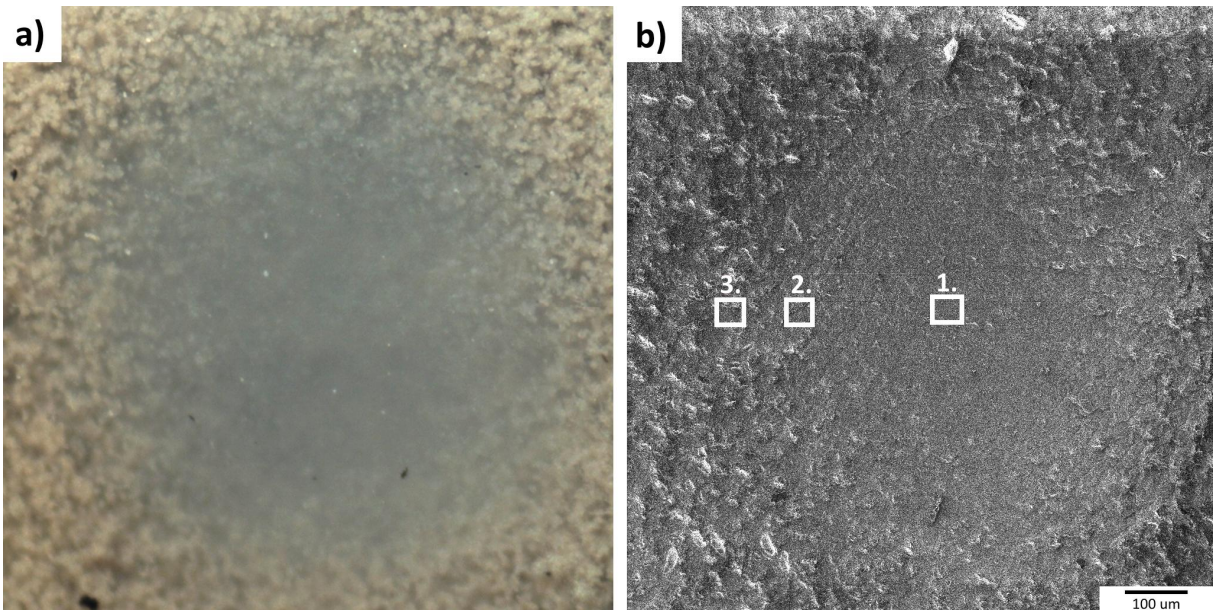

Figure 1. Images of a plaque formed by T4-infection in an *E. coli* lawn on an agar plate. The same plaque is shown here imaged with a) an optical microscope and b) with HIM. The areas investigated further in finer detail with HIM are shown with numbered squares.

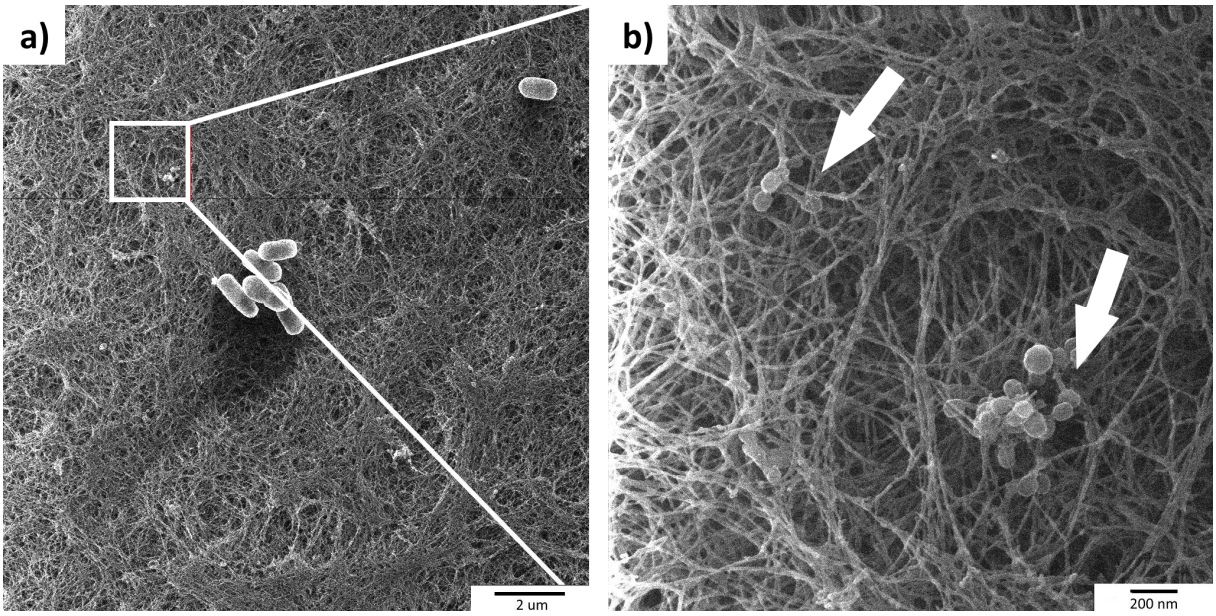

Figure 2. a) HIM image of area 1 in Figure 1b from the center of the plaque. Only few individual *E. coli* cells are visible. b) With a higher magnification T4 phages (arrows) can also be seen on the thin fibrous agar surface.

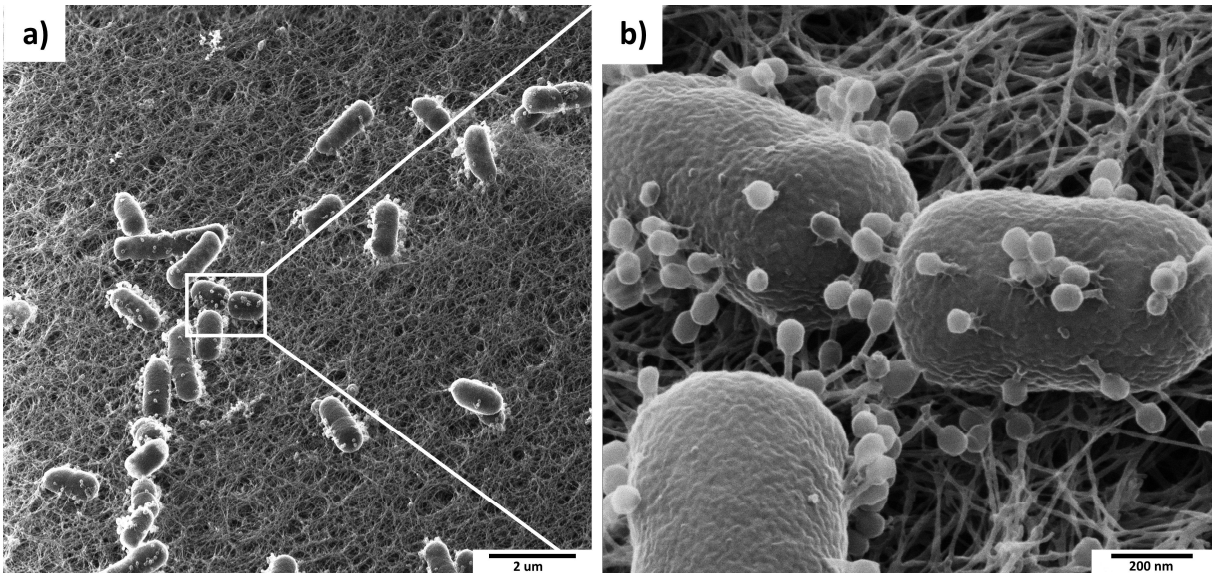

Figure 3. a) HIM image of area 2 in Figure 1b closer the edge of the plaque showing more bacterial cells with ongoing phage infections. b) Higher magnification of allows visualization of individual T4-phages attached onto the bacterial cell surface, some with contracted tails indicating genome injection. Free phages next to bacterial cells are also found.

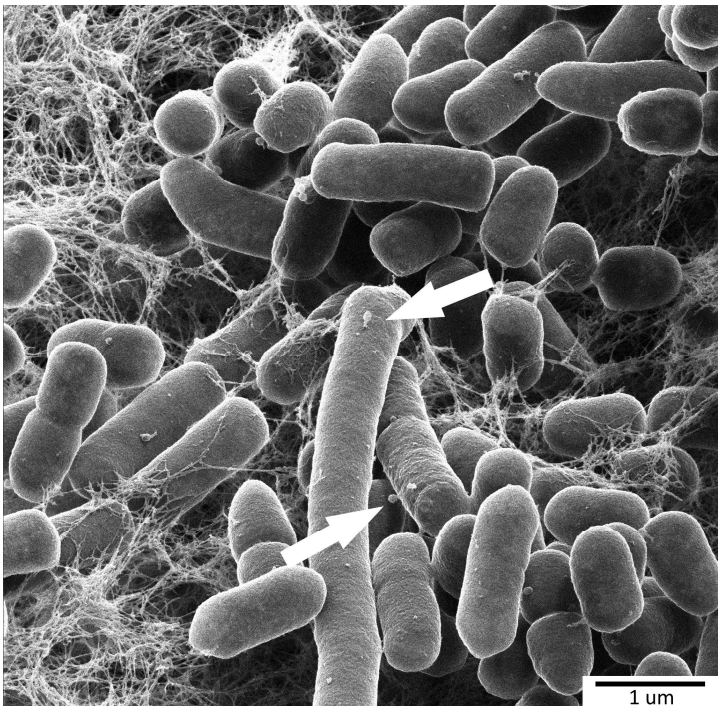

Figure 4. HIM image of area 3 in Figure 1b at the edge the plaque. The bacterial cells form microcolonies and few infecting phages are found (arrows).

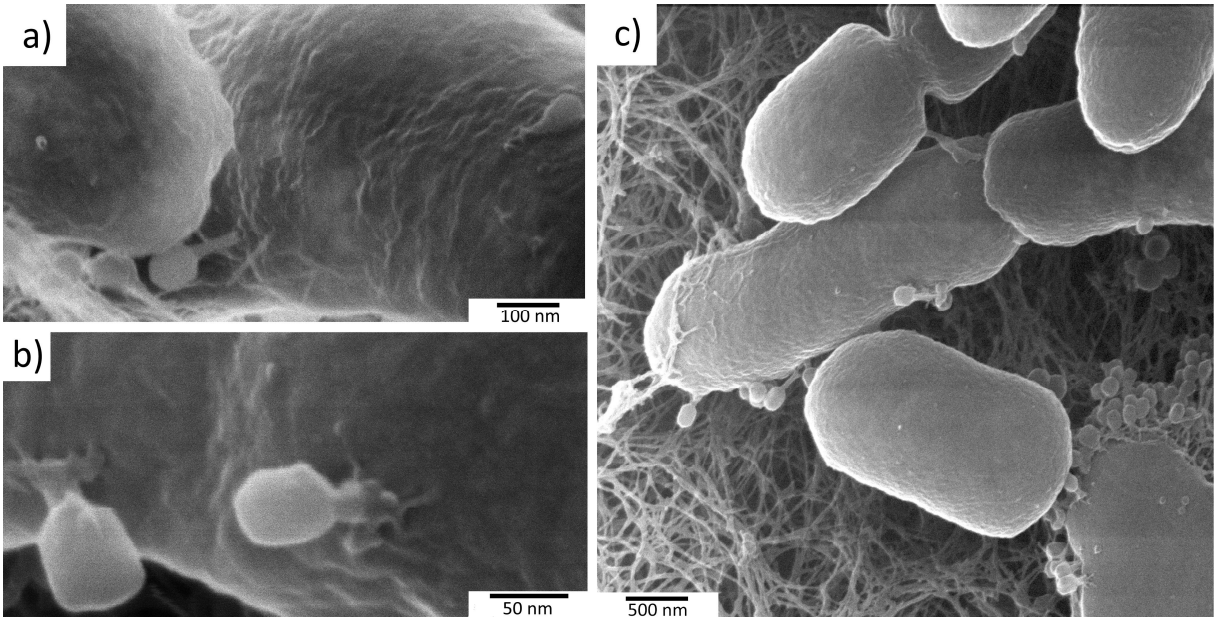

Figure 5. Visualization of the life cycle of a phage using HIM. a) A high resolution image of an early stage of the phage infection: T4 phage is attached on the surface of an *E. coli* bacterium. b) Several phages with contracted tails and spread out tail fibers indicating an active infection and genome injection. c) Lower right hand corner: Lysis of a bacterial cell and bursting out of a large number of new phage particles.

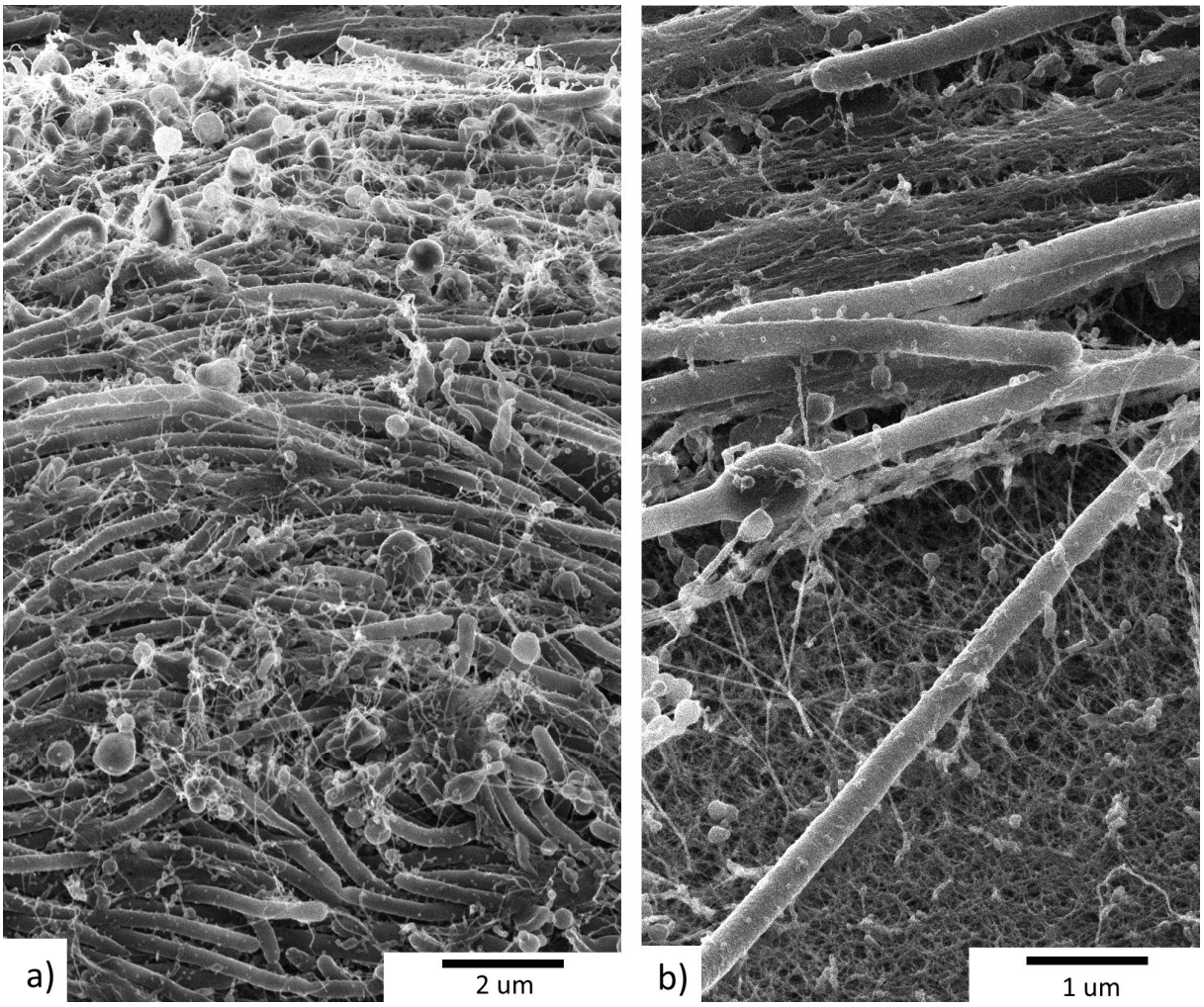

Figure 6. a) An image form a *Flavobacterium columnare* (B185) colony. A lot of extracellular vesicles and fibers are seen. b) A higher resolution image of an area where the contact between the colony and the agar substrate medium can be seen. Note the straight fibers connecting the cells to the substrate.

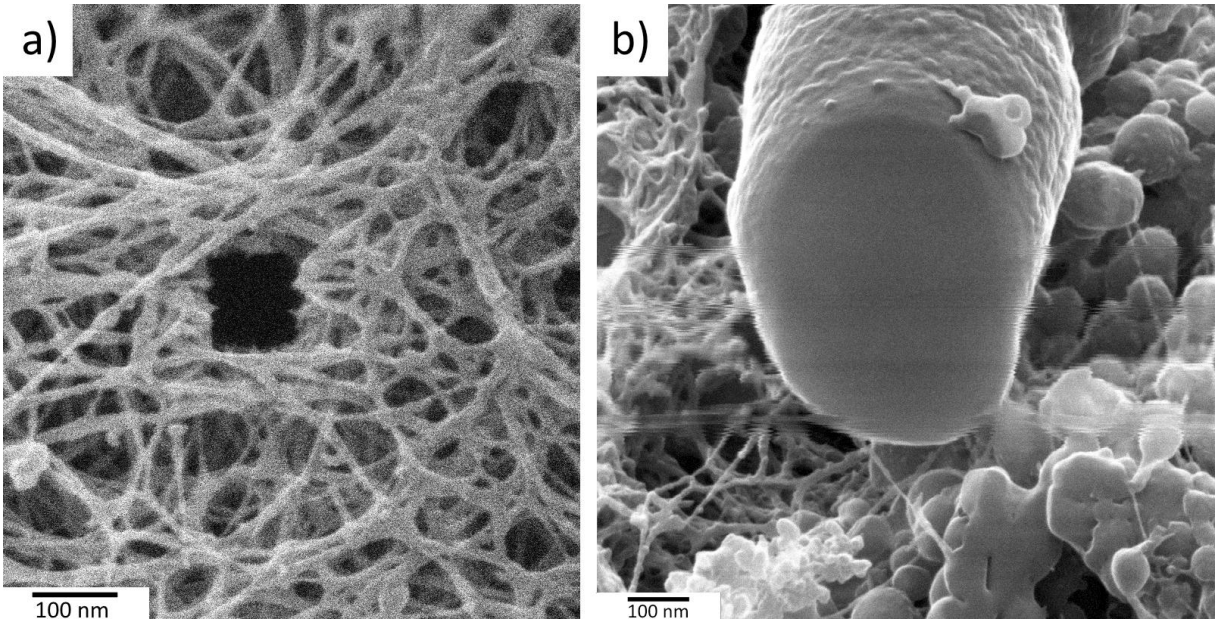

Figure 7. a) 100 x 100 nm area milled to the agar substrate with the flood gun on. b) He-milled bacteria showing up cut-off surface and a half-away cut phage particle on top of it. Milling was done from the 45º angle and imaging after 180º rotation.

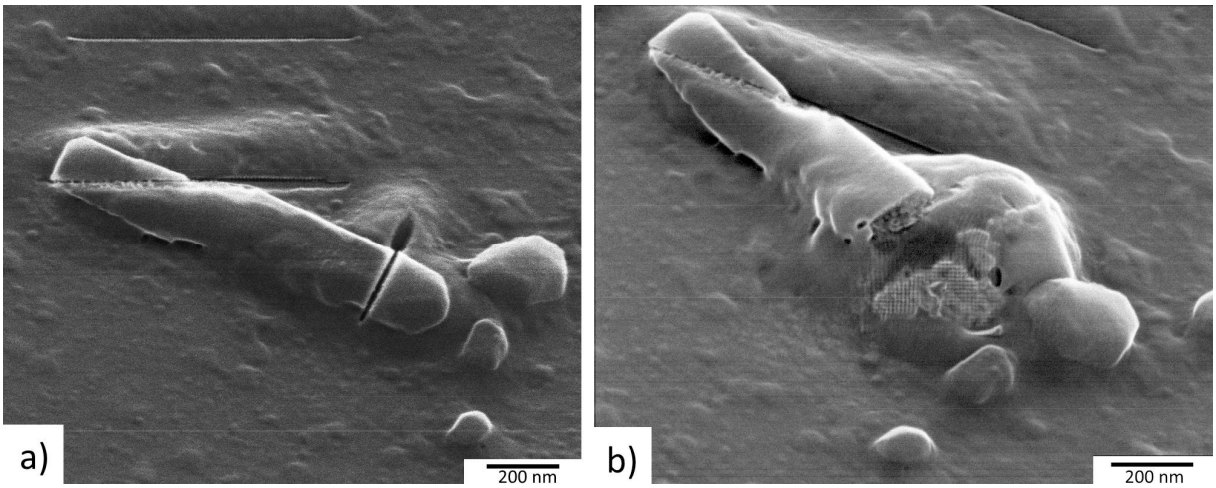

Figure 8. a) *Flavobacterium sp.* 183 after exposing line structures over its body. b) The same bacterium after the removal of the cut out "head" portion, revealing some inner structural details of the cell.

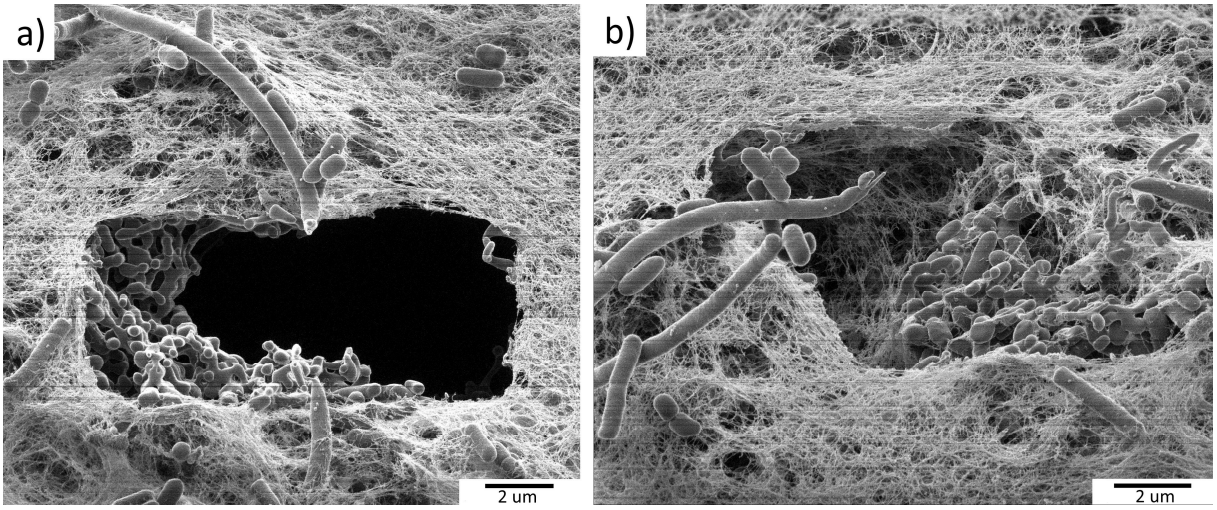

Figure 9. a) Slot milled to the agar substrate from an 45º angle with neon and imaged from 90 degree angle. b) The same milled area imaged with a 45º tilt and a 90º rotation.